Int J Clin Exp Med 2019;12(6):6901-6908
www.ijcem.com /ISSN:1940-5901/IJCEM0084363

Original Article

Modulation of colon cancer cell proliferation and invasion by MT1M via the NF-κB/VEGF signaling pathway

Kai Cheng[1], Youneng Yuan[1], Renhai Xiong[1], Yugang Cao[2]

Departments of [1]Gastrointestinal Surgery, [2]Hepatobiliary Surgery, Huangshi Central Hospital, Affiliated Hospital of Hubei Polytechnic University, Edong Healthcare Group, Huangshi 435000, Hubei, China

Received August 21, 2018; Accepted January 6, 2019; Epub June 15, 2019; Published June 30, 2019

Abstract: Colon cancer (CC) is a common malignant tumor of the digestive tract and is the third most popular cancer worldwide. MT1M is a member of MT family, and has been suggested to regulate tumors such as liver cancer, thyroid carcinoma, and cervical cancer. However, its expression or functional mechanism in CC remains unclear. Real-time PCR was performed for analysis of expression of MT1M mRNA in CC tissues and adjacent tissues. The cultured CC cell line SW620 was assigned into control and MT1M groups (transfected with MT1M plasmid) followed by analysis of MT1M expression by real-time PCR, cell proliferation by MTT assay, cell apoptosis by flow cytometry, and tumor invasion by Transwell chamber assay. Western blot measured expression of Bcl-2, Bax, NF-κB, and VEGF. MT1M was down-regulated in CC tissues ($P < 0.05$ compared to adjacent tissues). Transfection of MT1M plasmid into SW620 cells enhanced expression. The proliferation of SW620 cells was inhibited, accompanied with enhanced cell apoptosis and suppressed tumor invasion, plus higher Bax expression and decreased expression of Bcl-2, NF-κB, and VEGF ($P < 0.05$ compared to control group). In conclusion, MT1M is down-regulated in CC tissues and up-regulation of MT1M facilitates CC cell apoptosis and inhibits cancer proliferation and invasion possibly through modulating the NF-κB/VEGF signaling pathway.

Keywords: MT1M, colon carcinoma, NF-κB, VEGF, cell apoptosis, proliferation

Introduction

Colon carcinoma (CC) is a common malignant tumor of digestive tract, and mainly originates at the junction site between colon and rectum. With persisting high frequency, CC is the third popular cancer worldwide [1, 2]. With life style transition, and diet habit towards to more fatty acid, meat and salted food, plus environmental factors, CC incidence is continuously increased [3]. In China, the incidence of CC is rapidly increasing, with a younger patient population. However, the early screening, diagnosis, and prevention of CC have difficulty, leading to persistently high incidence of CC in China [4, 5]. Although continuous advancement of medical technique has diversified treatment approaches for CC including surgery, radiotherapy, chemotherapy and targeted treatment that can improve the treatment in an individualized manner, the overall treatment efficiency of CC has not been significantly improved [6, 7]. Onset and progression of CC involves multiple steps and factors. Genetic factors can lead to inflammatory change of normal colon epithelium, for progressively generation of colon adenoma and CC [8, 9]. The pathogenic mechanism for CC is complicated and has not been fully illustrated yet.

MT belongs to metal binding protein with lower molecular weight and is widely expressed in various tissues. MT sequence is enriched by cystine but without aromatic amino acids [10, 11]. Previous studies showed involvement of MT in tumor pathogenesis and progression [12]. MT1M is a member of metal sulfur protein family and modulates tumors including liver cancer, thyroid carcinoma and cervical cancer [13, 14]. However, its expression or functional role in CC remains poorly understood. The present study aims to investigate the expression profile of MT in CC.

Materials and methods

General information of patients

A total of 32 CC patients who were diagnosed as CC in the Department of Surgery in our hospital between January 2017 and December 2017 were recruited. All patients have received surgical treatment, aged between 39 and 69 years (average age = 45.2 ± 7.3 years). Tissues samples were collected during the surgery for pathological examination, subtyping and staging. Both tumor tissues and adjacent tissues (colon tissues more than 3 cm from tumor edge) were collected and stored in liquid nitrogen for further assays. All cases were diagnosed as primary CC by pathological examination. Exclusive and inclusive criteria [9]: Primary CC patients having not received surgery, chemo- or radio-therapy previously. Those patients conferring recurrent or metastatic CC, having received surgery, chemo- or radio-therapy, complicated with other disorders, systemic immune dysfunction, or complication of cancers, or those patients are not able to or unwilling to cooperate this study or its follow-up were excluded. This study has been approved by the medical ethics committee of our hospital. All participants signed informed consents with full knowledge to this study.

Major reagent and equipment

CC cell line SW620 (CCL-227™) was purchased from ATCC cell bank (US). DMEM medium, penicillin-streptomycin dual antibiotics was purchased from Hyclone (US). Fetal bovine serum (FBS), DMSO and MTT powder were purchased from Gibco (US). Trypsin-EDTA lysis buffer was purchased from Sigma (US). PVDF membrane was purchased from Pall Life Sciences (US). Western blot reagents were purchased from Beyotime Biotech (China). ECL reagent was purchased from Amersham Biosciences. Rabbit anti-human NF-κB monoclonal antibody, rabbit anti-human VEGF monoclonal antibody, rabbit anti-human Bax monoclonal antibody, rabbit anti-human Bcl-2 monoclonal antibody, and goat anti-rabbit horseradish peroxidase (HRP) conjugated IgG secondary antibody were purchased from Cell Signaling (US). RNA extraction kit and reverse transcription kit were purchased from Axygen (US). PCR amplification kit and PCR product purification kit were purchased from Promega (US). Plasmid extraction kit and restriction endonuclease were purchased from Roche (US). Annexin V-PI apoptotic assay kit was purchased from BD (US). Lipo2000 reagent was purchased from Invitrogen (US). Transwell chamber was purchased from Corning (US). Labsystem Version 1.3.1 microplate reader was purchased from Bio-rad (US). ABI 7700 Fast fluorescent quantitative PCR cycler was purchased from ABI (US). Ultrapure workstation was purchased from Sutai Purification (China). Sonic ultrasound rupture apparatus was purchased from Sonics (US). Melody C6 flowy cytometry was purchased from BD (US).

Grouping of CC cell line SW620

CC cell line SW620 kept in liquid nitrogen were resituated for passage and randomly assigned into two groups: control group receiving normal cell incubation, and MT1M group transfected with MT1M plasmid.

MT1M plasmid construction and cell transfection

MT1M sequence was designed by PrimerPremier 6.0 and inserted into pCMV plasmid. Primer sequences were: forward, 5'-ATTGC CGACC AATTC GGATG AACTG CTC-3'; reverse, 5'-ATTCG TCGAG CACAG CAGTC AGCTG-3'. Primers were synthesized by Gimma Biotech (China). Using clonal human CC cellular cDNA database as the template, pCMV-MT1M was used to construct cDNA containing restriction digestion site. Products were purified and digested by restriction nuclease for ligation into pCMV plasmid. Recombinant plasmid pCMV-MT1M was confirmed by dual restriction digestion and sequencing.

Real-time PCR for MT1M mRNA expression in CC tissues and SW620 cells

Trizol reagent was used to extract RNA from CC tissues, tumor adjacent tissues and SW620 cells from all groups. DNA reverse transcription was performed following the manual instruction of test kit. Primers were designed by PrimerPremier 6.0 and were synthesized by Invitrogen Biotech (China) as in **Table 1**. Real-time PCR was performed under the following conditions: 56°C 1 minute, followed by 35 cycles each consisting of 92°C 30 seconds, 60°C 45 seconds and 72°C 20 seconds. Data were collected and CT values of all samples and standards were calculated based on fluo-

Table 1. Primer sequence

Gene	Forward 5'-3'	Reverse 5'-3'
GAPDH	AGTACCAGTCTGTTGCTGG	TAATAGACCCGGATGTCTGGT
MT1M	TCCTCTGCTCCTACCTAGT	TGGGATTGTTGGTGTTTGTATA

rescent quantification and using GAPDH as the reference. Using CT values of standards as the reference, a standard curve was plotted for semi-quantitative analysis using $2^{-\Delta Ct}$ approach.

Western blot for protein expression of Bcl-2, Bax, NF-κB and VEGF

Proteins were extracted from all groups of SW-620 cells. In brief, RIPA lysis buffer containing proteinase inhibitor was added for cell lysis for 15~30 minutes on ice. Cells were ruptured by ultrasound treatment (5 seconds, 4 times), and cell lysate was centrifuged under 4°C with 10000 g for 15 minutes. The supernatant was saved and proteins were quantified by Bradford approach. Proteins were separated on 10% SDS-PAGE, and transferred to PVDF membrane using semi-dry method (230 mA, 2 hours). Non-specific binding background was removed using 5% defatted milk powder for 2 hours at room temperature incubation. Primary antibody (Bcl-2 at 1:2000, Bax at 1:1000, NF-κB at 1:1000 or VEGF at 1:2000) was added for overnight incubation at 4°C. The next day, the membrane was rinsed in PBST, and 1:2000 diluted goat anti-rabbit secondary antibody was added for dark incubation at room temperature for 30 minutes. The membrane was developed using ECL reagent for 1 minute, followed by X-ray exposure. Protein imaging processing software and Quantity One system were used to scan X-ray film and to measure band densities. All experiments were repeated for four times (n = 4) for statistical analysis.

MTT assay for cell proliferation

SW620 cells at log-growth phase were inoculated into 96-well plate at a density of 5×10^3 cells per well using DMEM medium containing 10% FBS. After 24 hour incubation, the supernatant was discarded. Cells were randomly assigned into two treatment groups as above-mentioned. Each well was filled with 20 μl sterile MTT after 48 hour incubation. Triplicated wells were set for each treatment group. After 4 hour continuous incubation, the supernatant was removed and 150 μl DMSO was added into each well followed by 10 minutes vortex. After complete resolving of crystal violet, absorbance (A) values were measured at 570 nm wavelength in a microplate reader. The proliferation rate of all groups was calculated and each experiment was repeated for more than three times.

Cell apoptosis assay

Culture medium of all groups was discarded, and attached cells were rinsed by pre-cold PBS. Cells were then digested and rinsed at 1000 rpm for 5 minutes using 1X PBS. Cells were fixed in 75% pre-cold ethanol for overnight incubation at 4°C. After discarding 75% ethanol, cells were rinsed in 1X PBS at 1000 rpm for 5 min, and were resuspended in 800 μl 1X PBS mixed with 1% BSA. After adding 100 μg/ml PI staining buffer (3.8% sodium citrate, pH7.0) and 100 RnaseA (10 mg/ml), cells were incubated in dark for 30 minutes at 37°C. Then 300 μl of 1X Binding buffer was added into the cell mixture and cell apoptosis was measured by flow cytometry.

Transwell chamber assay

Transwell assay was used to measure cell invasion following the manual instruction of test kit. In brief, serum-free DMEM medium was used for 24 hour incubation. Transwell chamber was pre-coated with 50 mg/L Matrigel dilution buffer (1:5) on its bottom and upper membrane. After 4°C air-drying, 500 μl DMEM medium containing 10% FBS and 100 μl serum-free DMEM medium prepared tumor cell suspensions were added into interior and exterior of the chamber, respectively. Triplicated wells were set for each group, and the chamber was placed into 24-well plate. Control group included Transwell chamber without Matrigel. After 48 hour incubation, the Transwell chamber was rinsed by PBS and cells on the membrane was removed followed by cold ethanol fixation. After staining in crystal violet, cells on the lower phase of the membrane were enumerated. Each experiment was repeated three times.

Statistical processing

All data are presented as mean standard ± standard deviation (SD). Comparison of means

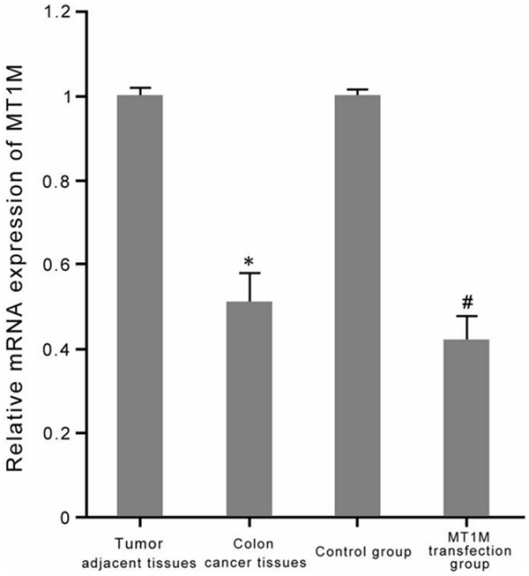

Figure 1. Expression of MT1M in CC tumor tissues and cells. *P < 0.05 comparing to tumor adjacent tissues; #P < 0.05 comparing to the control group.

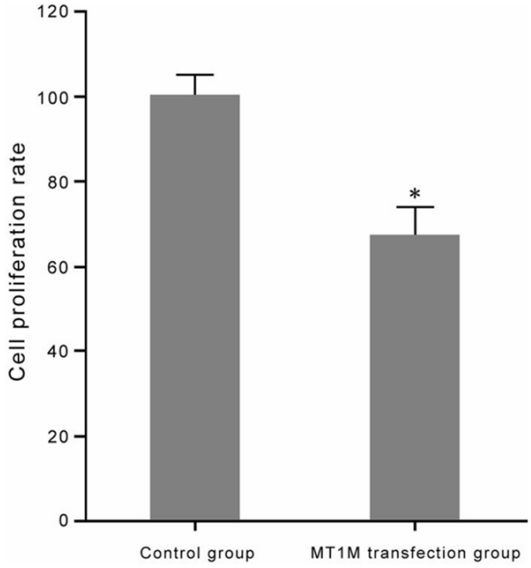

Figure 2. Effects of MT1M on proliferation of CC cell line SW620. *P < 0.05 comparing to the control group.

between two groups was performed by student t-test. SPSS 11.5 software was used for statistical analysis. Comparison among groups was revealed by analysis of variance (ANOVA). Enumeration was analyzed by χ^2 test. Pearson correlation analysis was employed for correlation analysis. A statistical significance was defined when P < 0.05.

Results

Expression of MT1M in CC tumor tissues and cells

Real-time PCR was used to measure expression of MT1M and showed significantly enhanced MT1M mRNA expression in CC tumor tissues (P < 0.05 compared to adjacent tissues). Transfection of MT1M plasmid into CC cells remarkably increased MT1M mRNA expression (P < 0.05 compared to the control group, **Figure 1**).

Effects of MT1M on CC cell line SW620 proliferation

MTT assay was used to test the effect of MT1M transfection on proliferation of CC cell line SW620. Results showed that transfection of MT1M for 48 hours significantly inhibited proliferation of CC cell line SW620 (*P* < 0.05 compared to the control group, **Figure 2**), suggesting that MT1M exerts prominent inhibitory role on SW620 cell proliferation.

Effect of MT1M on apoptosis of CC cell line SW620

Flow cytometry was used to test the effect of MT1M transfection for 48 hours on the apoptosis of CC cell line SW620 and found that 48 hour transfection of MT1M significantly induced apoptosis of CC cell line SW620 (*P* < 0.05 compared to control group, **Figure 3**), indicating that MT1M could induce apoptosis of the CC cell line SW620.

Effect of MT1M on invasion of CC cell line SW620

Transwell chamber was used to measure the effect of 48 hour MT1M transfection on invasion potency of CC cell line SW620. Results showed that transfection of MT1M for 48 hours significantly inhibited invasion potency of CC cell line SW620 (*P* < 0.05 compared to the control group, **Figure 4**), revealing that MT1M has a prominent inhibitory role on invasion of CC cell line SW620.

Effects of MT1M on apoptosis/anti-apoptosis

Western blot was used to analyze the effect of 48 hour MT1M transfection on the expression

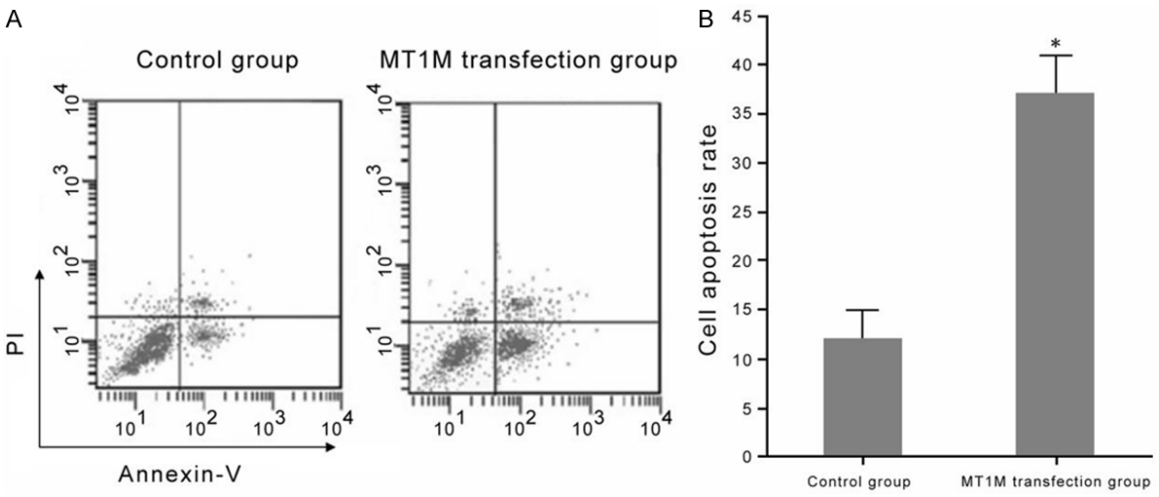

Figure 3. Effects of MT1M on CC cell line SW620 apoptosis. A. Flow cytometry to measure the effect of MT1M on CC cell line SW620 apoptosis. B. Analysis of CC cell line SW620 apoptosis. *P < 0.05 comparing to the control group.

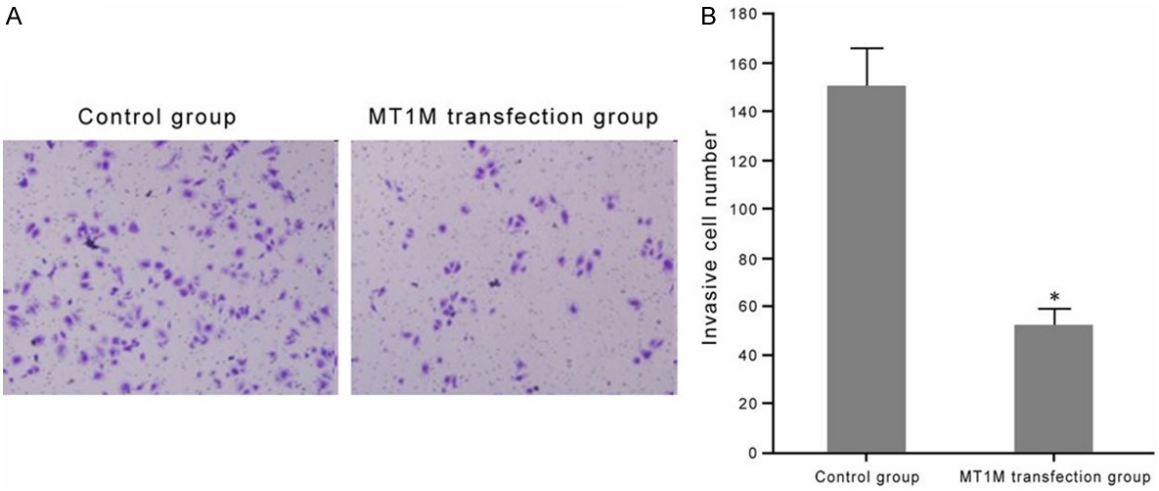

Figure 4. Effect of MT1M on invasion of CC cell line SW620. A. Transwell chamber assay for the effect of MT1M on the invasion of CC cell line SW620. B. Analysis for the effect of MT1M on SW620 cell invasion. *P < 0.05 comparing to the control group.

of apoptotic/anti-apoptotic proteins in CC cell line SW620. Results showed that 48 hour transfection of MT1M transfection significantly facilitated Bax expression and decreased Bcl-2 expression ($P < 0.05$ compared to control group, **Figure 5**).

Effect of MT1M on NF-κB/VEGF signal pathway of CC cell line SW620

Western blot was used to analyze the effect of 48 hour MT1M transfection on the NF-κB/VEGF signaling pathway in CC cell line SW620. Results showed that transfection of MT1M into CC cell line SW620 significantly inhibited NF-κB or VEGF expression ($P < 0.05$ compared to the control group, **Figure 6**).

Discussion

MT is highly conserved and consists of four isoforms from MT-1 to MT-4, with wide distribution in mammalian body [15, 16]. MT can detoxify heavy metal poison such as zinc or cesium. It can enhance body resistance via modulating body adaption toward heavy metals or unfavorable environment, and can assist trafficking of trace elements, thus exerting crucial roles in

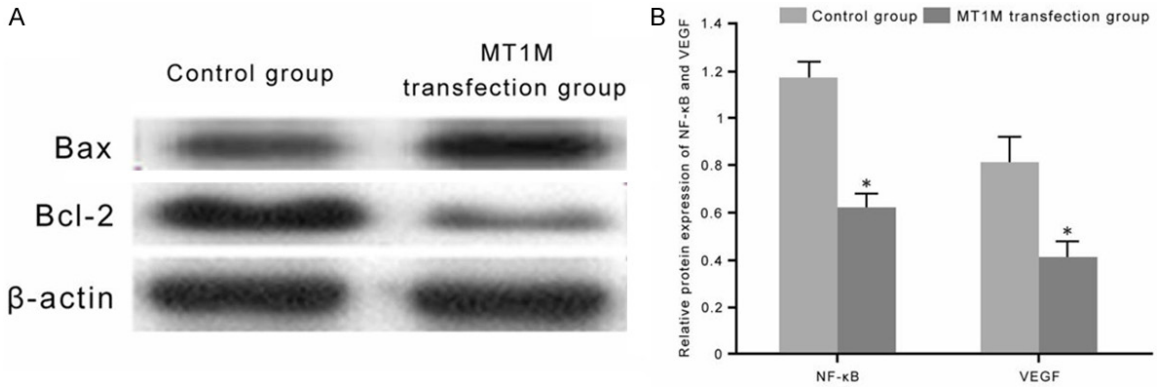

Figure 5. Effect of MT1M on apoptosis/anti-apoptosis of CC cell line SW620. A. Western blot analysis for the effect of MT1M on apoptosis/anti-apoptosis of CC cell line SW620. B. Analysis of the effect of MT1M on expression of proteins related with apoptosis/anti-apoptosis in CC cell line SW620. *P < 0.05 comparing to the control group.

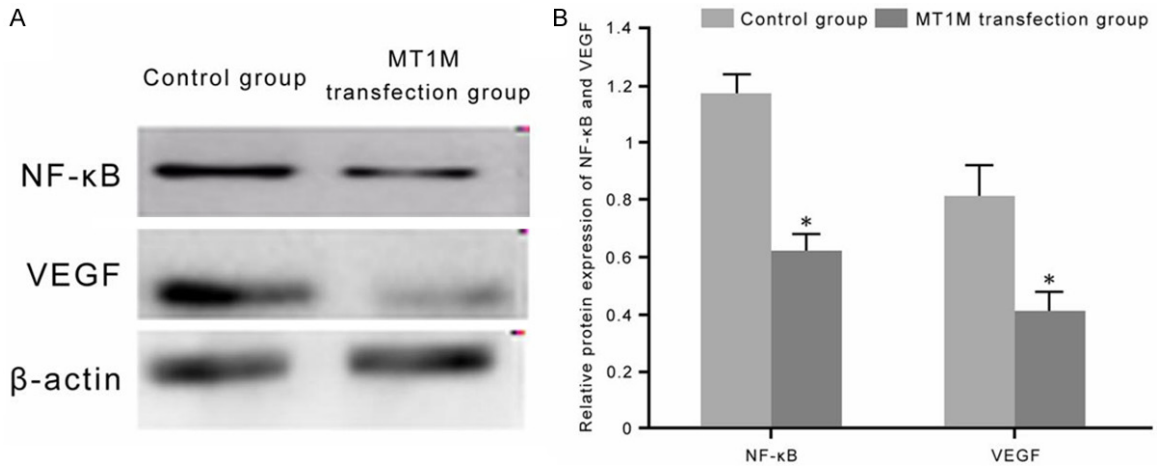

Figure 6. Effects of MT1M on the NF-κB/VEGF signaling pathway. A. Western blot for the effect of MT1M on the NF-κB/VEGF signaling pathway of CC cell line SW620. B. Analysis for the effect of MT1M on the NF-κB/VEGF signaling pathway of CC cell line SW620. *P < 0.05 comparing to the control group.

clearance of free radicals [17]. MT1M gene belongs to MT-1 subtype. Clinical studies confirmed that MT1M played important roles in tumor cell modulation. For example, MT1M down-regulation was observed in thyroid cancer cells and breast cancer tissues, thus facilitating tumor cell growth and proliferation [18]. Therefore, MT1M has promising perspectives to become a potential novel target for tumor treatment. However, expression of MT1M in CC tissues or related mechanism has not been elucidated yet. This study thus constructed a eukaryotic expression plasmid of MT1M gene, which was transfected into CC cells to investigate the effect of MT1M on CC cell biological behavior. In the present study, transfection of CC cell line SW620 with the MT1M gene significantly inhibited CC cell proliferation. Further studies on apoptosis or invasion of CC cell line SW620 demonstrated that transfection of SW620 cells by MT1M gene could facilitate tumor cell apoptosis and inhibit invasion. These results demonstrate that the MT1M gene could enhance the inhibitory role on proliferation and invasion of CC cell line SW620, to facilitate tumor cell apoptosis for further modulating tumor occurrence and progression.

Cell apoptosis plays crucial roles in modulating onset and progression of CC [19]. Cell apoptosis refers to the kind of homeostatic control of the body including inhibition of tumor overgrowth and retarding tumor metastasis. Overexpression of Bcl-2 expression and apoptotic

protein Bax down-regulation are closely associated with imbalanced apoptosis/anti-apoptosis homeostasis of liver cancer cells [20]. In addition, nuclear factor NF-κB has also been demonstrated to participate in tumor pathogenesis [21]. Vascular endothelial growth factor (VEGF) plays roles in tumor angiogenesis, tumor proliferation and invasion, and tumor progression possibly through modulating NF-κB/VEGF pathway [22, 23]. Therefore, the functional mechanism was further investigated and it was found that MT1M inhibits the NF-κB/VEGF signaling pathway, suppresses Bcl-2 and potentiates Bax expression. However, the current study still has limitations such as relatively smaller sample size that requires further large cohort clinical study. Moreover, further mechanistic studies are required to provide evidence for clinical demonstration of MT1M as a therapeutic target for the treatment of tumors.

Conclusion

MT1M is down-regulated in CC tumor tissues. Up-regulation of MT1M modulates expression of apoptosis/anti-apoptosis proteins possibly via modulating the NF-κB/VEGF signaling pathway.

Disclosure of conflict of interest

None.

Address correspondence to: Dr. Yugang Cao, Department of Hepatobiliary Surgery, Huangshi Central Hospital, Affiliated Hospital of Hubei Polytechnic University, Edong Healthcare Group, No. 141, Tianjin Road, Huangshi 435000, Hubei, China. Tel: +86-0714-6222922; Fax: +86-0714-6222922; E-mail: xiongcheng102kg@126.com

References

[1] Weber D, Amar L, Godde D and Prinz C. Extensive screening of microRNA populations identifies hsa-miR-375 and hsa-miR-133a-3p as selective markers for human rectal and colon cancer. Oncotarget 2018; 9: 27256-27267.

[2] Smid M, Coebergh van den Braak RRJ, van de Werken HJG, van Riet J, van Galen A, de Weerd V, van der Vlugt-Daane M, Bril SI, Lalmahomed ZS, Kloosterman WP, Wilting SM, Foekens JA, JNM IJ, Martens JWM and Sieuwerts AM. Gene length corrected trimmed mean of M-values (GeTMM) processing of RNA-seq data performs similarly in intersample analyses while improving intrasample comparisons. BMC Bioinformatics 2018; 19: 236.

[3] Reichert CL, Silva DB, Carollo CA, Weffort-Santos AM and Santos CA. Metabolic profiling and correlation analysis for the determination of killer compounds of proliferating and clonogenic HRT-18 colon cancer cells from Lafoensia pacari. J Ethnopharmacol 2018; 224: 541-552.

[4] Chen X, Guan H, Liu XD, Xie DF, Wang Y, Ma T, Huang B and Zhou PK. p53 positively regulates the expression of cancer stem cell marker CD133 in HCT116 colon cancer cells. Oncol Lett 2018; 16: 431-438.

[5] Neilsen BK, Chakraborty B, McCall JL, Frodyma DE, Sleightholm RL, Fisher KW and Lewis RE. WDR5 supports colon cancer cells by promoting methylation of H3K4 and suppressing DNA damage. BMC Cancer 2018; 18: 673.

[6] Han B, Cao YX, Li ZM, Wu ZX, Mao YQ, Chen HL, Yao ZJ and Wang LS. Annonaceous acetogenin mimic AA005 suppresses human colon cancer cell growth in vivo through downregulation of Mcl-1. Acta Pharmacol Sin 2019; 40: 231-242.

[7] Okonkwo A, Mitra J, Johnson GS, Li L, Dashwood WM, Hegde ML, Yue C, Dashwood RH and Rajendran P. Heterocyclic analogs of sulforaphane trigger DNA damage and impede DNA repair in colon cancer cells: interplay of HATs and HDACs. Mol Nutr Food Res 2018; e1800228.

[8] Klobucar M, Grbcic P, Pavelic SK, Jonjic N, Visentin S and Sedic M. Acid ceramidase inhibition sensitizes human colon cancer cells to oxaliplatin through downregulation of transglutaminase 2 and beta1 integrin/FAK-mediated signalling. Biochem Biophys Res Commun 2018; 503: 843-848.

[9] Uribe G, Villeger R, Bressollier P, Dillard RN, Worthley DL, Wang TC, Powell DW, Urdaci MC and Pinchuk IV. Lactobacillus rhamnosus GG increases COX-2 expression and PGE2 secretion in colonic myofibroblasts via a MyD88-dependent mechanism during homeostasis. Cell Microbiol 2018; 20: e12871.

[10] Klaren WD, Flor S, Gibson-Corley KN, Ludewig G and Robertson LW. Metallothionein's role in PCB126 induced hepatotoxicity and hepatic micronutrient disruption. Toxicol Rep 2016; 3: 21-28.

[11] Tomas M, Tinti A, Bofill R, Capdevila M, Atrian S and Torreggiani A. Comparative Raman study of four plant metallothionein isoforms: Insights into their Zn(II) clusters and protein conformations. J Inorg Biochem 2016; 156: 55-63.

[12] Kubo T, Kuroda Y, Horiuchi S, Kim SR, Sekino Y and Ishida S. Upregulations of metallothionein gene expressions and tolerance to heavy metal toxicity by three dimensional cultivation of

HepG2 cells on VECELL 3-D inserts. J Toxicol Sci 2016; 41: 147-53.
[13] AlGhamdi S, Leoncikas V, Plant KE and Plant NJ. Synergistic interaction between lipid-loading and doxorubicin exposure in Huh7 hepatoma cells results in enhanced cytotoxicity and cellular oxidative stress: implications for acute and chronic care of obese cancer patients. Toxicol Res (Camb) 2015; 4: 1479-1487.
[14] Ji XF, Fan YC, Gao S, Yang Y, Zhang JJ and Wang K. MT1M and MT1G promoter methylation as biomarkers for hepatocellular carcinoma. World J Gastroenterol 2014; 20: 4723-9.
[15] Mao J, Yu H, Wang C, Sun L, Jiang W, Zhang P, Xiao Q, Han D, Saiyin H, Zhu J, Chen T, Roberts LR, Huang H and Yu L. Metallothionein MT1M is a tumor suppressor of human hepatocellular carcinomas. Carcinogenesis 2012; 33: 2568-77.
[16] Somparn A, Iwai CB and Noller B. Potential use of acetylcholinesterase, glutathione-S-transferase and metallothionein for assessment of contaminated sediment in tropical chironomid, Chironomus javanus. J Environ Biol 2015; 36: 1355-9.
[17] Eidizadeh A, Khajehalichalehshtari M, Freyer D and Trendelenburg G. Assessment of the therapeutic potential of metallothionein-ii application in focal cerebral ischemia in vitro and in vivo. PLoS One 2015; 10: e0144035.
[18] Nowinska K, Chmielewska M, Piotrowska A, Pula B, Pastuszewski W, Krecicki T, Podhorska-Okolow M, Zabel M and Dziegiel P. Correlation between levels of expression of minichromosome maintenance proteins, Ki-67 proliferation antigen and metallothionein I/II in laryngeal squamous cell cancer. Int J Oncol 2016; 48: 635-45.
[19] Liu Q, Si T, Xu X, Liang F, Wang L and Pan S. Electromagnetic radiation at 900 MHz induces sperm apoptosis through bcl-2, bax and caspase-3 signaling pathways in rats. Reprod Health 2015; 12: 65.
[20] Borghetti G, Yamaguchi AA, Aikawa J, Yamazaki RK, de Brito GA and Fernandes LC. Fish oil administration mediates apoptosis of Walker 256 tumor cells by modulation of p53, Bcl-2, caspase-7 and caspase-3 protein expression. Lipids Health Dis 2015; 14: 94.
[21] Ng KL, Yap NY, Rajandram R, Small D, Pailoor J, Ong TA, Razack AH, Wood ST, Morais C and Gobe GC. Nuclear factor-kappa B subunits and their prognostic cancer-specific survival value in renal cell carcinoma patients. Pathology 2018; 50: 511-518.
[22] Chao WH, Lai MY, Pan HT, Shiu HW, Chen MM and Chao HM. Dendrobium nobile Lindley and its bibenzyl component moscatilin are able to protect retinal cells from ischemia/hypoxia by dowregulating placental growth factor and upregulating Norrie disease protein. BMC Complement Altern Med 2018; 18: 193.
[23] Huang CY, Lee CH, Tu CC, Wu CH, Huang MT, Wei PL and Chang YJ. Glucose-regulated protein 94 mediates progression and metastasis of esophageal squamous cell carcinoma via mitochondrial function and the NF-kB/COX-2/VEGF axis. Oncotarget 2018; 9: 9425-9441.